Field Extraction from Near Field Scanning for a Microstrip Structure

Lin Zhang, Kevin P. Slattery*, Chen Wang, Masahiro Yamaguchi, Ken-Ichi Arai**, Richard E. DuBroff, James L. Drewniak, David Pommerenke, and Todd Hubing**

Electromagnetic Compatibility Laboratory

Department of Electrical and Computer Engineering

University of Missouri-Rolla

Rolla, MO. 65409 (lzhang@umr.edu)

*Intel Desktop Architecture Lab

Hillsboro, OR 97124 (kevin.p.slattery@intel.com)

**Research Institute of Electrical Communication (RIEC)

Tohoku University

Sendai, Japan (yamaguti@riec.tohoku.ac.jp)

Abstract

Currents associated with high-speed digital devices have significant impacts on EMI problems in VLSI design and operation. In this paper, a simple transmission line model was implemented as an initial step to represent the EMI mechanisms associated with an IC package. Numerical modeling results were compared with near field scanning measurements and show that the magnetic field deduced from the measurements agrees well with the numerical predictions.

Keywords

Numerical modeling, Microstrip, Near field scanning.

INTRODUCTION

A near field scanning system is used to observe the magnetic fields associated with these signals as the frequency of the signal varies. Over different frequency ranges, various unintentional coupling paths may be provided by frequency-dependent parasitics, and this should be reflected in the magnetic field pattern observed by the near field scanner at various frequencies.

MODELING STRATEGY

To investigate the near-zone fields, a microstrip structure comprised of two parallel microstrip transmission lines was constructed. Each of the two lines had a port at each end. At each of the four ports, the center conductor of an SMA jack was connected to the line and the shield was connected to the ground plane. Figure 1 provides a schematic representation of the twin microstrip structure.

The dimension of the structure was 111 mm × 147 mm × 1.17 mm. The dielectric was FR4. The width of each microstrip line was 6 mm, and the length was 106 mm. The distance between the two lines was 12 mm. The two lines were located in the center area of the board. The near end ports are visible in this schematic view but the far end ports are not. Ports 1 though 4 correspond respectively to the near end of line 1, the far end of line 1, the far end of line 2 and the near end of line 2, as shown in Figure 1. Measured results were obtained using a network analyzer (HP8753D) driving port 1 of the microstrip structure while the remaining ports were terminated with 50Ω resistive loads. Port 2 of the network analyzer was connected to a small loop probe controlled by the near field scanning mechanism.

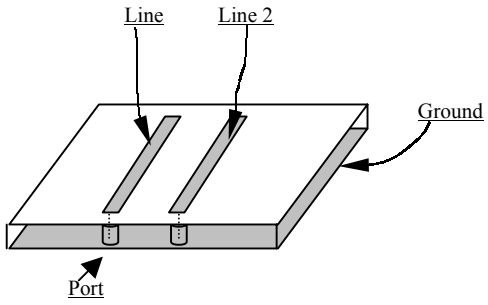

Figure 1. Overview of the test structure.

Numerical results were obtained using finite difference time domain (FDTD) numerical modeling to predict the electromagnetic fields surrounding the microstrip structure. In numerical modeling, the structure was meshed by cells having dimensions of 0.5 mm × 0.5 mm × 0.234 mm. The total number of the cells was 222 × 294 × 5.

Validation of the FDTD modeling results consisted of comparing the S11 parameter measured by the network analyzer with the S11 parameter as calculated using the FDTD program. Figure 2 shows the results of this comparison over a frequency range from 1 MHz to 3 GHz.

From Figure 2 the low frequency agreement between modeled and measured results is good but the agreement is not

0-7803-7264-6/02/$17.00 © 2002 IEEE

quite as good at higher frequencies. A comparison of the phase of S11, measured and modeled, although not shown here did demonstrate a similar pattern of agreement--good at low frequencies and worse at high frequencies.

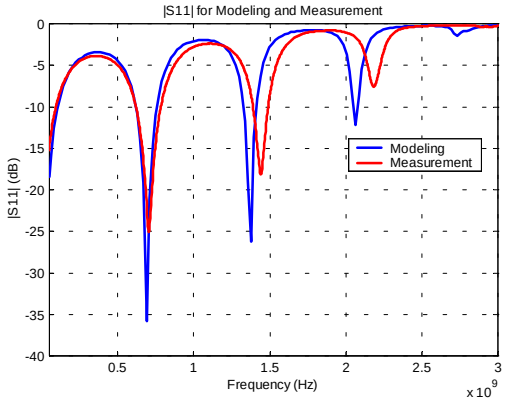

Figure 2. Comparison of S11 magnitude.

In subsequent discussions of modeled and measured results reference will be made to a coordinate system in which the y axis runs parallel to the microstrip traces and the z axis extends from the reference plane to the traces, as shown in Figure 3, below.

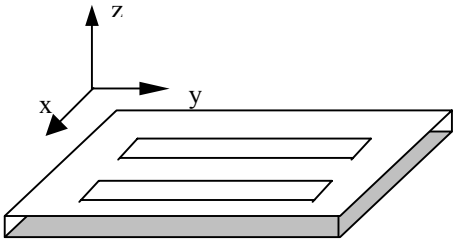

Figure 3. Coordinate system used in describing modeled and measured results.

The measured and modeled S11 magnitudes indicate a resonance at around 2 GHz. This seems to correlate well with the frequency at which the modeled current on trace 1 obtains its maximum value as shown in Figure 4.

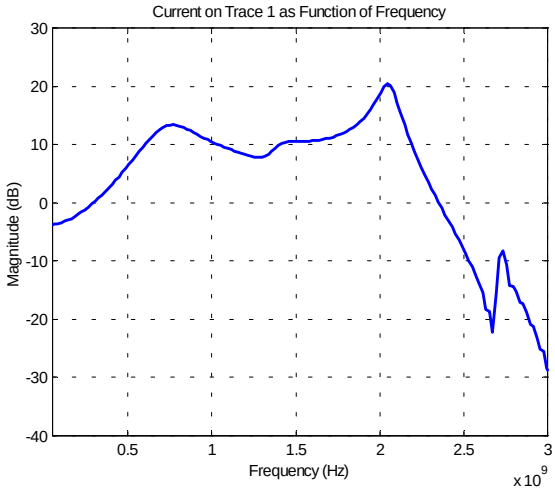

Figure 4. Spectrum of current at y = 45 mm.

A similar result, which is shown in Figure 5, was obtained for the modeled current at y = 33cm. This point corresponds to the current at port 1.

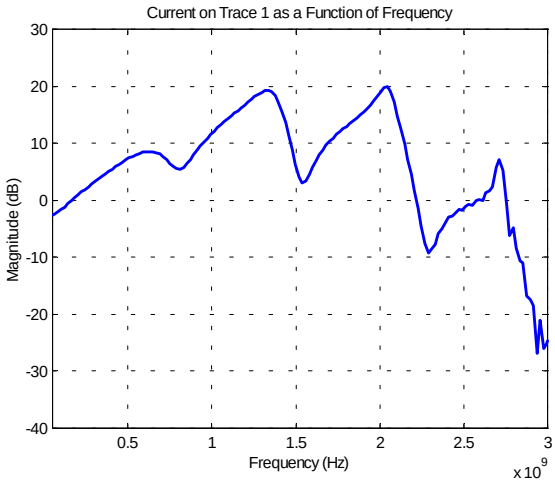

Figure 5. Spectrum of current at y = 33 mm.

S21 MEASUREMENT SETUP

An automated xy scanning system was used in connection with an HP8753D vector network analyzer to measure the variation of S21 over the region above each microstrip line. Figure 6 illustrates a small loop probe connected to the scanning system and located in proximity to the two microstrip lines. Measurements were made for both horizontal orientations of a small loop probe. In one case the loop probe was oriented with its normal direction parallel to the x axis and in the other case it was oriented with its normal direction parallel to the y axis.

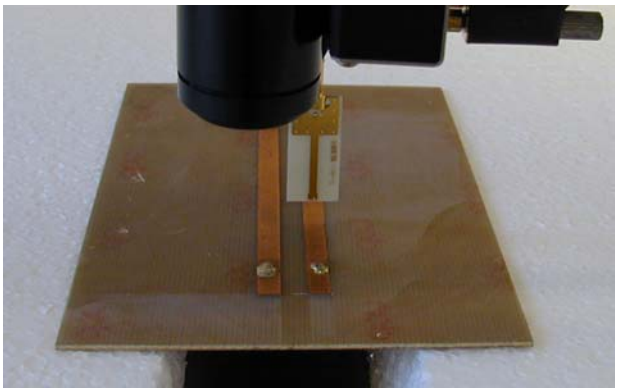

Figure 6. A small loop probe driven by an automated mechanical near field scanning system.

COMPARISON OF MODELING AND MEASUREMENT RESULTS FOR S21

In the ideal case of probes that introduce no loading and respond proportionately to the field intensity at each point above each microstrip trace, the magnitude of S21 in the measurements should be proportional to the magnitude of the corresponding field component in the numerical simulation.

Therefore, in the following figures the measured values of the magnitude of S21 are compared with the numerically simulated magnetic field.

In each case the data is presented as the variation in the modeled (measured) magnetic field component, in dB, versus location over one of the two microstrip traces. To allow for the possiblity of unresolved constants of proportionality in converting the loop probe's output into a field component magnitude, only the relative variation of the modeled and measured field components should be compared. A constant number of decibels was added to the measured result in each of the following five figures and this constant vertical offset was determined by eye, rather than by any experimental measurement or analysis. Also all of the following comparisons between measured and modeled values were done for a frequency of 2.05 GHz corresponding to the dominant response in Figures 2, 4, and 5.

The first example, Figure 7, shows a comparison between the modeled and measured magnetic field components in the x direction.

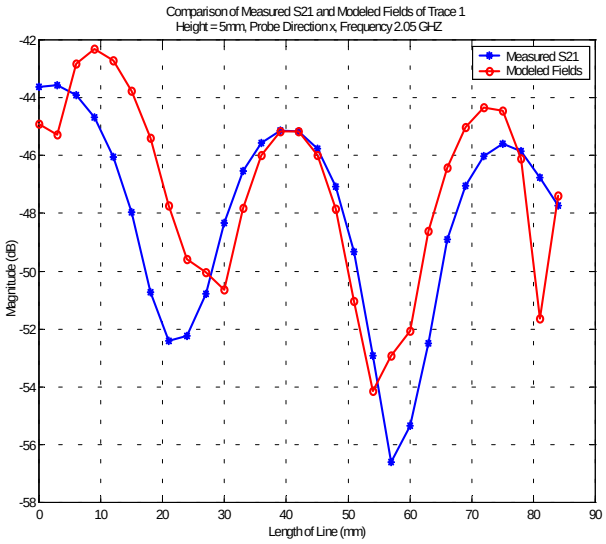

Figure 7. Case I: Comparison of modeled and measured magnetic field at 5 mm above Trace 1.

The following comparison, Figure 8, shows the same measured and modeled field components at a distance of 10 mm over trace 1.

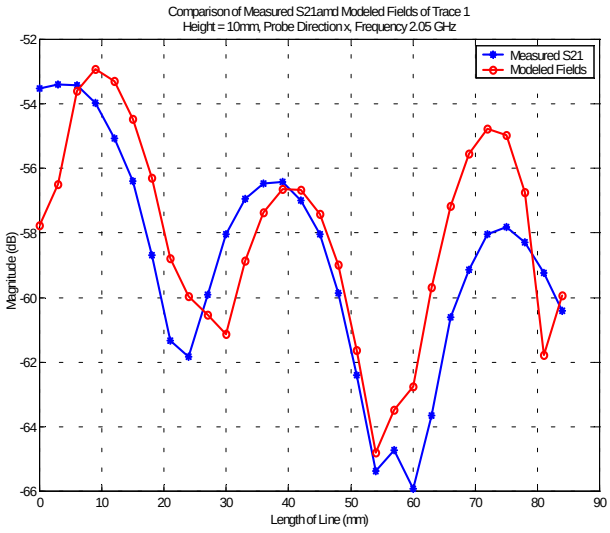

Figure 8. Comparison for a 10mm height over Trace 1.

The variation of the magnetic fields in this case is very similar to the variation in the previous case.

Figure 9 shows a comparison of the modeled and measured magnetic field distribution over Trace 2. In this case the general pattern is similar but the agreement is not as close as in the case of the driven trace (Trace 1).

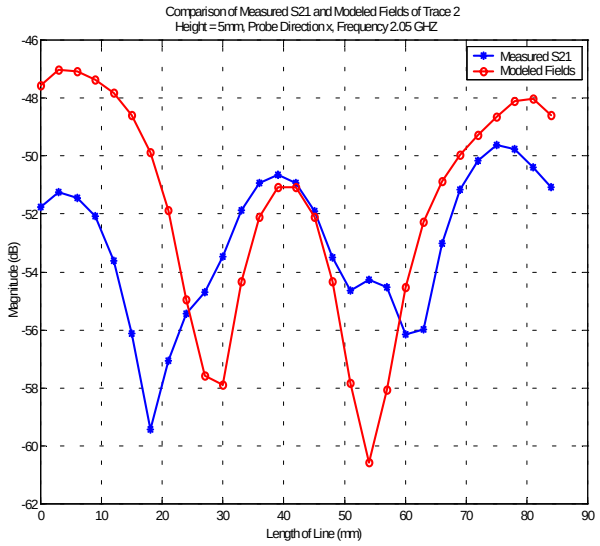

Figure 9. Comparison for a 5mm height over Trace 2.

Figure 10 compares the magnetic field components in the y direction at a vertical distance of 5 mm above trace 1.

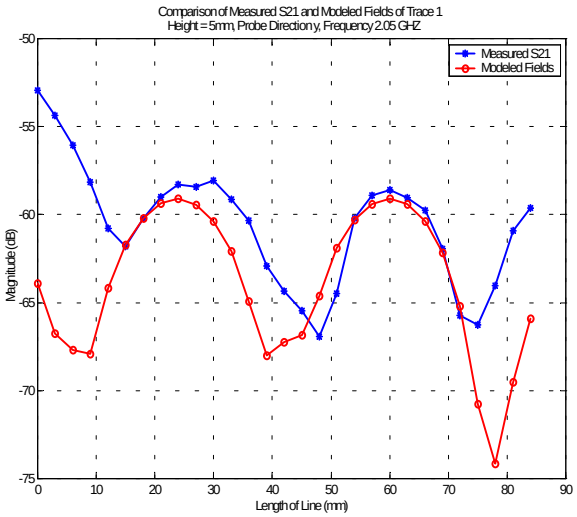

Figure 10. Comparison of the y components at 5 mm over Trace 1.

Finally Figure 11 compares y components of the modeled and measured magnetic fields over trace 2, again at a vertical offset distance of 5 mm.

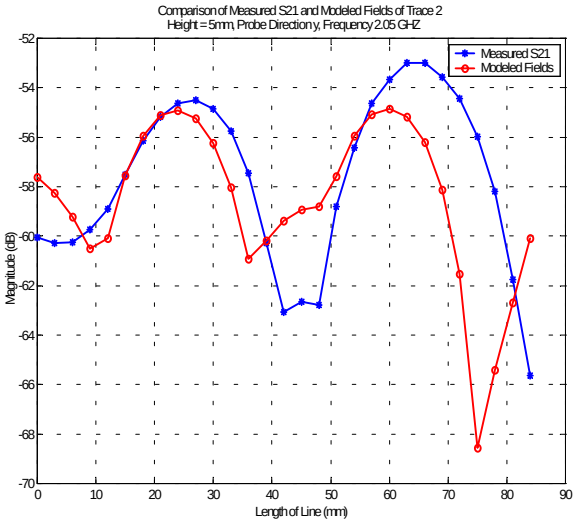

Figure 11. Comparison of the y components at 5 mm over Trace 2.

CONCLUSION

The near field scanning has resulted in a set of measured magnetic field magnitudes that are in general agreement with the results of numerical modeling. Several explanations are possible for the residual discrepancy between the two sets of results. Non-ideal probe properties whereby the probe's receiving characteristics are not consistent with the simple proportional model considered here provides one possible explanation. The numerical modeling also could be the cause of some discrepancy. In particular, the comparison of S11 magnitudes in Figure 2 made no use of the near field scanning probes. Yet there was a clear discrepancy between the numerical result and the result provided by the network analyzer. Moreover, the discrepancy in the location of S11 minima seemed to become progressively worse as the frequency increased. A similar frequency dependent discrepancy was noticed in the phase of S11. These discrepancies could suggest that the parameters used in the FDTD model were perhaps not adequate over the entire frequency range. Therefore, it is possible that a better agreement in S11 (by adjusting the FDTD parameters) might lead to a better agreement in the field component comparison.

REFERENCES

[1] R. R. Goulette, "The Measurement of Radiated Emissions from Integrated Circuits", IEEE 1992 International Symposium, Electromagnetic Compatibility, 1992. Page: 340 –345.

[2] David M. Pozar, *Microwave Engineering*, 2rd ed., John Wiley & Sons, Inc, 1998.

[3] SAE J1752-2, "Measurement of Radiated Emissions from ICs Surface Scan Method", 2000.